Accepted Manuscript

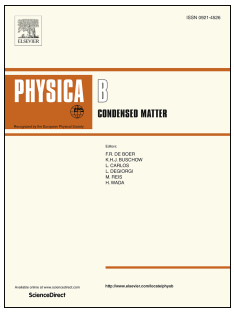

Critical behaviour of microemulsions: Monte Carlo simulations of Widom model

Edgar A. Bea, Marta L. Trobo, Andres De Virgiliis

PII: S0921-4526(18)30656-2

DOI: https://doi.org/10.1016/j.physb.2018.10.029

Reference: PHYSB 311115

To appear in: *Physica B: Physics of Condensed Matter*

Received Date: 28 June 2018

Revised Date: 17 September 2018

Accepted Date: 18 October 2018

Please cite this article as: E.A. Bea, M.L. Trobo, A. De Virgiliis, Critical behaviour of microemulsions: Monte Carlo simulations of Widom model, *Physica B: Physics of Condensed Matter* (2018), doi: https://doi.org/10.1016/j.physb.2018.10.029.

Critical behaviour of microemulsions: Monte Carlo simulations of Widom model

Edgar A. Bea[a], Marta L. Trobo[a,b], Andres De Virgiliis[a,b,*]

[a] *Instituto de Física de Líquidos y Sistemas Biológicos (IFLYSIB), CCT-CONICET La Plata, Calle 59 789, B1900BTE La Plata, Argentina*

[b] *Departamento de Ciencias Básicas, Facultad de Ingeniería, Universidad Nacional de La Plata, Argentina*

Abstract

The critical behaviour of a lattice model for ternary mixtures of hydrophilic, hydrophobic and amphiphilic (surfactant) molecules is investigated by means of Monte Carlo simulations. A lattice model formulated by Widom as a simple approach of these mixtures is adopted taking advantage of its equivalence to a spin-$\frac{1}{2}$ Ising model, which adds next nearest neighbors interactions on a simple cubic lattice. In this work we focus on the critical behaviour of the order-disorder phase transition of this model. A simulation strategy combining a standard Metropolis sampling and multiple histogram reweighting technique is used. The location of the phase boundary is well determined, being consistent with the 3D Ising critical temperature. In addition, a suitable finite size scaling analysis is performed to obtain critical amplitudes of magnitudes as magnetization, susceptibility and interfacial tension. The critical behaviour results compatible with the 3D Ising universality class, as expected. Likewise, critical amplitudes ratios give a reasonable agreement with the universal values obtained from different systems and methods.

Keywords: Ternary mixture, Lattice model, Phase transition, Monte Carlo simulation, Finite size scaling

*Corresponding author
Email address: adevir@iflysib.unlp.edu.ar (Andres De Virgiliis)

1. Introduction

It is well known that binary mixtures of water and oil are immiscible because the interfacial tension between them is large making it energetically impossible to create huge interfaces by thermal fluctuations. However, if amphiphiles (surfactant) are introduced it can be drastically reduced because of the self-assembling ability of them organizing the other two components. The surfactant has the ability to dissolve immiscible liquids [1] favoring the formation of invisibly small droplets [2, 3] or more complex microemulsions.

Ternary mixtures of hydrophilic or polar molecules (water), hydrophobic or non-polar molecules (oil), and amphiphiles (polar and non-polar) have a rich thermodynamic behaviour. The study of these mixtures is motivated by its technological and economical importance since they are involved in processes such as assisted oil recovery, chemical synthesis, nanoparticle fabrication, and drug transport [4]. The most common use is in cleaning and removal of contaminants due to its exceptional capacity as a solubilizer favoring the detergency phenomenon. In addition, they also generate interest from a more fundamental point of view as they involve self-assembly processes and exhibit diverse critical phenomena such as phase separation or wetting transitions [5].

These mixtures have been studied generically by means of simplified microscopic models such as lattice models for fluids [6]. There are several lattice models for microemulsions in the literature [2, 3, 7, 8, 9, 10, 11, 12, 13, 14], and among them there are formulations based on spin-1 [12, 13, 14] and spin-$\frac{1}{2}$ [2, 3] variables. The simplest lattice model is proposed by Widom [2, 3] which is based on the spin-$\frac{1}{2}$ Ising model on a simple cubic lattice. In this model the interfacial energy vanishes at the stability limit of the ordered phase at low temperatures, as is required for an appropriate description of microemulsions. The behaviour of this magnitude is key and in this model there is no much quantitative data about it. Likewise, the interfacial tension is important because it gives an indication of the strength of capillary waves [15].

The Widom model has been extensively studied using mean field theory, which

allowed to derive direct although qualitatively the topology of the phase diagram [16, 17]. On the other hand, low-temperature series expansion techniques have also been applied to estimate the behaviour of the interfacial tension [18, 19].

In the phase diagram four kinds of phases were identified: water(oil)-rich, disordered fluid and lamellar phases. The transition between the disordered fluid and the lamellar phases is first order, while that between the disordered fluid and the oil-rich and water-rich phases is continuous. Because of this continouos transition, there is no three-phase coexistence between rich phases and disordered fluid, a fact that is contrary to experiment. The microemulsion phase is identified with the disordered fluid in that part of the phase diagram in which the water-water correlation function oscillates with a decaying amplitude, which is a signature of a structured fluid [20]. This behaviour is separated from the less structured fluid displaying correlations that decay monotonically through a disorder line which does not intersect the phase boundary between disordered and water- and oil-rich phases. In this manner, the microemulsion coexists only with the lamellar phase.

As any Ising-like system, the Widom model is particularly suitable for studies based on computer simulations. In that sense, it is striking that there are no recent studies by means of Monte Carlo simulations [18, 21, 22, 23]. Jan and Stauffer [21] performed simulations for bulk and interface systems in both square and simple cubic lattices. Their findings are in qualitative agreement with the mean field predictions, specially in the low temperature region of the phase diagram.

In this work we investigate the critical behaviour of the order-disorder phase transition of the Widom model based on Monte Carlo simulations. A simulation strategy combining a single-spin flip Metropolis sampling and a multiple histogram reweighting technique [24] is used for an improved description of physical magnitudes of interest around the phase boundary. Standard finite size scaling methods are then used to extrapolate to the thermodynamic limit and to determine critical amplitudes assuming the 3D Ising criticality. These critical

amplitudes are then used to test the universality of some ratios that have been estimated from previous theoretical and experimental works on related systems [25, 26, 27].

We first present a brief review of the critical behaviour of Ising-like systems in section 2. Next, we introduce the Widom model and describe the simulation technique in section 3. Then we present and discuss our results in section 4. Finally, we expose our conclusions in section 5.

2. Critical behaviour of Ising-like systems

In Ising-like lattice models, the phase diagram have a (second-order) continuous order-disorder phase transition and thermodynamic variables such as magnetization, susceptibility and interfacial tension have a critical behaviour.

Asumming hyperscaling, valid for systems that belong to the 3D Ising universality class, critical exponents and amplitudes of the associated power laws are [25, 26, 27]:

$$m = Bt^{\beta}, \quad \sigma = \sigma_0 t^{2\nu}, \quad \chi = \Gamma^{\pm}(\mp t)^{-\gamma}, \tag{1}$$

where t is a measure of distance from the critical point given by

$$t = \frac{M}{M^*} - 1, \tag{2}$$

by varying the temperature T or the spin coupling parameter M, being M^* its critical value. Note that the habitual symbol nomenclature has been preserved. The critical amplitudes are of interest because certain critical amplitude ratios are predicted to be universal. This universality implies that only two amplitudes are required to determine the remaining ones.

As the critical point is approached from the (ordered) two-phase region ($M>M^*$), m and σ vanish. Instead, χ diverges from both sides and its critical amplitudes are different (Γ^+ and Γ^-).

The critical exponents appropriate for Ising-like systems are the 3D Ising exponents. In the context of this work, we use β=0.324, γ=1.239 and ν=0.629.

Among the universal combinations of critical amplitudes [25, 26, 28], the following ratios are of importance [27]:

$$\frac{\Gamma^+}{\Gamma^-} \approx 4.76 \pm 0.24, \tag{3}$$

$$\frac{\sigma_0^{3/2}\Gamma^-}{B^2} \approx 0.13 \pm 0.04, \tag{4}$$

$$\frac{\sigma_0^{3/2}\Gamma^+}{B^2} \approx 0.71 \pm 0.13, \tag{5}$$

where $k_B T$ is used as the unit of energy. The ranges represent the spread in different estimates obtained from experiment, simulation and theory.

2.1. Finite size scaling

Those critical power laws cannot be observed directly in a single computer simulation since the correlation length diverges at critical point and hence cannot be captured in a finite system of size L. The correct approach must be made through of several simulations at different system sizes and using the predictions of finite size scaling theory to extrapolate to the thermodynamic limit [29, 30, 31].

In this section, we will only reproduce the equations required for our analysis. All thermodynamic magnitudes are derived from a probability distribution $P_L(m, e)$ as a function of the order parameter m and energy e, as will be well described later.

2.1.1. Magnitudes m and χ

The magnetization is derived of the probability distribution $P_L(m)$ as a function of the order parameter only, integrating over all energy range. It is identified as the mean position of the peaks.

According to finite size scaling theory, close to the critical point, the magnetization m_L for a finite system size L shows a systematic L-dependence that can be written as

$$m_L = L^{-\beta/\nu}\mathcal{M}^0(tL^{1/\nu}), \tag{6}$$

with critical exponents $\{\beta, \nu\}$ and a system size-independent scaling function $\mathcal{M}^{0}$. Whether the assumed universality class is indeed correct, scaling plots [30] $m_{L} L^{\beta/\nu}$ versus $tL^{1/\nu}$ should all collapse onto one master curve, provided the correct value of the critical system parameter (M^{*}) is used. Moreover, for large $tL^{1/\nu}$ (but still within the critical region) such plots should approach the power law behaviour of the thermodynamic limit. The mater curve of scaling plots in a double logarithmic scale should approach a straight line with slope β and intercept equal to B.

In relation to the susceptibility, it is identified as the variance of the peaks in the probability distribution $P_{L}(m)$. In (ordered) two-phase region, we define the susceptibility as

$$\chi_{L}^{f} = \frac{1}{L^{3}} \left(\int_{-L^{3}}^{L^{3}} m^{2} P_{L}(m)\, dm - \langle m \rangle^{2} \right), \tag{7}$$

while in (disordered) one-phase region, the distribution looses its bimodal structure and becomes single peaked, thus in this regime the correct definition for the susceptibility reads

$$\chi_{L}^{p} = \frac{1}{L^{3}} \int_{-L^{3}}^{L^{3}} m^{2} P_{L}(m)\, dm. \tag{8}$$

In the case, the scaling behaviour of the susceptibility is given by

$$\chi_{L} = L^{\gamma/\nu} \chi^{0}(tL^{1/\nu}). \tag{9}$$

In the master curve of scaling plots, the straight line has slope -γ and intercept equal to $\Gamma^{\pm}$, depending on whether the critical point is approached from the two-phase region (Γ^{-}) or one-phase region (Γ^{+}).

2.1.2. Magnitude σ

The interfacial tension σ_{L} is defined from the free energy of the system for a finite system size L and it is obtained from the logarithm of the probability distribution of the order parameter, W=$\ln P_{L}(m)$, see Fig. 1. This function corresponds to the free energy of the system so that the height of the peaks in

W can be identified as the free energy of the water-rich and oil-rich phases. The free energy barrier F_L separating these two symmetrical phases (i.e. both peaks should have the same height) is then calculated from W through the difference F_L=$W(+)$-$W(0)$ in Fig. 1.

The interfacial tension for the finite system of size L reads (in d dimensions) [32]

$$\sigma_L = \frac{F_L}{2L^{d-1}}, \tag{10}$$

where the factor of two is introduced to take into account the formation of two interfaces in the system due to the use of periodic boundary conditions.

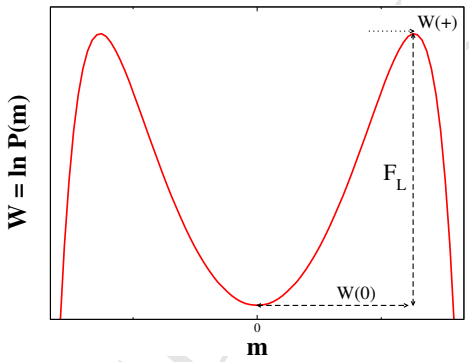

Figure 1: Logarithm of the probability distribution W=ln $P_L(m)$ for the magnetization of the Widom model in the ferromagnetic phase. The peak $W(+)$ corresponds to an ordered phase of up spins (*water*-rich phase), while the $W(-)$ peak for m<0 corresponds to the phase of down spins (*oil*-rich phase). $W(0)$ is the minimum value between the two peaks. The free energy barrier (F_L) separates the two phases in equilibrium for a system size L.

Since we are interested in the critical behaviour of the interfacial tension at the thermodynamic limit (σ_∞), we note it is connected to the free energy barrier F_L by the expression [27]

$$\exp(F_L) = aL^x \exp(2L^{d-1}\sigma_\infty). \tag{11}$$

After taking logarithm on both sides of this expression one gets

$$\sigma_L = \sigma_\infty + \frac{x \ln L}{2L^{d-1}} + \frac{\ln a}{2L^{d-1}}, \tag{12}$$

where the constants (a, x) are not known. We apply equation 12 to extrapolate our data obtained for finite sizes L to the thermodynamic limit. Following the prescription of Ref. [32], we have directly excluded the second term $\ln L/L^{d\text{-}1}$ from Eq. 12 because the range of simulated system sizes is relatively small and therefore it is difficult to separate numerically.

3. Model and simulation method

The Widom model [2, 3] is isomorphic to a spin-$\frac{1}{2}$ Ising model, with spin variables S_i=±1, where bonds between spin pairs represent three types of molecules according to the net spin state of the i-th pair, S_i+S_{i+1}={−1,0,+1}, in such a way that a pair of parallel spins represent either water (+1,+1) or oil (−1,−1), while every pair of antiparallel spins (+1,−1) represents surfactant. By this construction, each spin on the cubic lattice system belongs to six such pairs. This implies that oil and water must always be separated by a surfactant. The Ising Hamiltonian describing the total interaction energy contains pair coupling terms comprising to first, second and fourth nearest neighbors:

$$\mathcal{H} = -J \sum_{<i,j>} S_i S_j - 2M \sum_{<i,k>} S_i S_k - M \sum_{<i,l>} S_i S_l \qquad (13)$$

where the first sum is over all nearest neighbor pairs, the second sum is over all next-nearest neighbor pairs, and the third sum goes over all pairs of neighbors which are two lattice distances apart (i.e. fourth-neighbors). On the cubic lattice, each site has 6 nearest neighbors (J), 12 next-nearest neighbors ($2M$), and 6 distance = 2 neighbors (M). The two coupling constants J>0 and M<0 are related to the interaction between surfactants and the chemical potential. The competition between those interactions leads to the characteristic behaviour observed in microemulsions: phases of complex structure, a high osmotic compressibility, and a low interfacial tension.

We consider here the simplest case in which oil and water have equal chemical potential corresponding to equal energies for the amphiphile sheet to bend toward water or to oil. In the Ising magnet language this case is equivalent to a

zero bulk magnetic field. Even in its simplified version, the Widom model stills shows a rich phase diagram.

We simulate the Widom model described by the Hamiltonian of Eq. 13 by performing Monte Carlo simulations on simple cubic lattices of edge length L under periodic boundary conditions. The single spin flip Metropolis algorithm is employed. Simulations are done at selected values of the coupling constant $J/k_{B}T \equiv J_{k}$ and varying the other coupling constant $M/k_{B}T \equiv M_{k}$ in the neighborhood of the order-disorder transition. Every simulation starts from a completely disordered spin configuration.

For a finite system size L and selected values of coupling parameters $\{J_{k}, M_{k}\}$, (total) energy and order parameter data of the simulation in equilibrium are collected in a histogram representing directly the probability $P_{L}(m, e)$ of observing the order parameter m and energy e in the system. These distributions are normalized to unity.

We employ the multiple histogram reweighting method [24] to extrapolate the probability distributions. A number of physical observables such as the magnetization, susceptibility and interfacial tension are derived from the order-parameter probability $P_{L}(m)$, which results from integrating $P_{L}(m, e)$ over all energy range. The standar finite size scaling theory [31] is used to characterize the phase transition by a careful analysis of the critical behaviour of such magnitudes.

4. Results and discussion

We systematically explore the order-disorder phase transition line in a J_{k}-range which includes the 3D Ising critical point (for M=0, J_{k}) and extend up to the neighborhood of the Widom model tricritical point [16], *i.e.* $0.15 \leq J_{k} \leq 0.90$. For the finite size analysis we use simulation box sizes L ranging from 10 up to 20. The Metropolis relaxation period was around $2 \cdot 10^{6}$ to $8 \cdot 10^{6}$ Mote Carlo steps (MCS). After relaxation, an additional period is simulated for data collection

of 10^6 to $5{\cdot}10^7$ MCS. For every combination of the parameters $\{J_k, M_k\}$, eight statistically independent simulations using different random seeds are employed.

Next we present all the information divided in several sections according to the kind of results.

4.1. Probability distribution $P(m, e)$

Fig. 2 shows the probability distributions $P_L(m, e)$ corresponding to selected values of the coupling parameter M_k around the critical point for J_k=0.15. Simulated systems in this region of the phase diagram only have ferromagnetic couplings at first and next nearest neighbors, so that a behaviour similar to the Ising model is expected. As can be seen, as the critical point is approached from two-phase region the distribution loses its bimodal structure and becomes single peaked. This transition to the (disordered) one-phase region occurs at a critical temperature higher than that of the Ising model, J_k<0.22, because the ferromagnetic field is reinforced by the contribution of next-nearest neighbor spins (M_k>0).

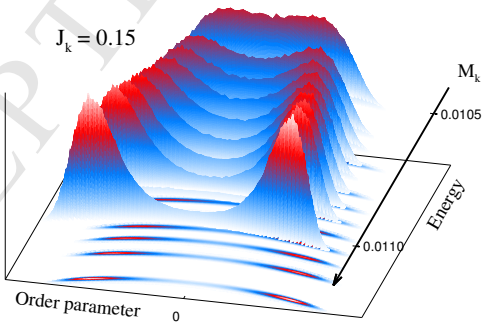

Figure 2: Probability distribution $P_L(m, e)$ for selected M_k values surrounding the critical point of the order-disorder phase transition for J_k=0.15. The data result from Monte Carlo simulations for systems of size L=20.

4.2. Universal Ising distribution

As already said before, Widom model belongs to the 3D Ising universality class. That means that the probability distribution $P_L(m)$ must collapse onto a characteristic *universal* distribution at a point $\{J_k, M_k\}$ on any exploration path of the phase transition. This point giving the best collapse corresponds to a critical point on the phase transition line.

Figure 3 shows the best collapse of $P_L(m)$ for J_k=0.25 and different system sizes L. Critical M_k values are extrapoled to the thermodynamic limit by plotting them as a function of $L^{-1/\nu}$, see inset in Fig. 3. For the case shown, J_k=0.25, the resulting M_k^* is -0.0040805(5).

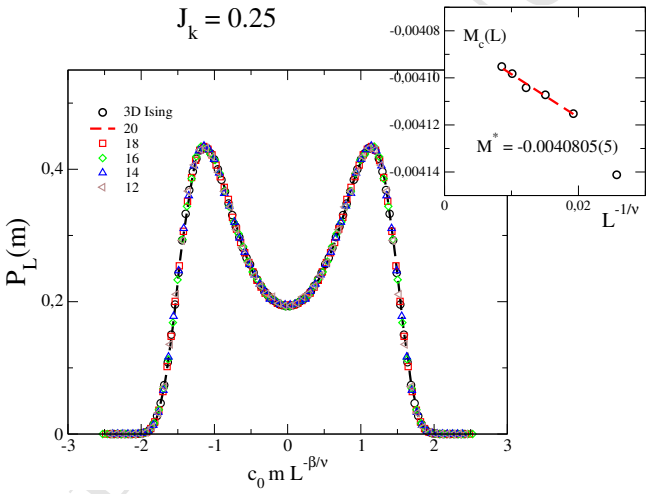

Figure 3: Best collapse of the probability distribution $P_L(m)$ with the universal Ising distribution for J_k=0.25 and different system sizes L. Inset shows the finite size behaviour of critical M_k values giving the best collapse and the extrapolation at thermodynamic limit. c_0 is a non-universal constant.

Usually cumulant intersection method [33] is used to estimate the location of the critical point. It takes advantage of the finite size scaling of the distribution $P_L(m)$ as it collapses to the universal Ising distribution at critical point, intersecting all distribution moments there. However, in this work we estimate it by searching for the best collapse of distributions $P_L(m)$. Table 1 exhibits

the critical M_k values for the J_k values analyzed.

Table 1: Critical M_k values for the J_k values analyzed corresponding to the order-disorder phase transition of the Widom model. Each M_k^* results from extrapolating to the thermodynamic limit the M_k values giving the best collapse of the probability distribution $P_L(m)$ with the universal Ising distribution.

J_k	M_k^*
0.15	0.0107744
0.20	0.0034197
0.25	-0.0040805
0.33	-0.0154939
0.40	-0.0245473
0.50	-0.0376547

4.3. Phase boundary

In Fig. 4 we collect onto a single plot our results for the J_k values analyzed (Table 1). Data taken from previous works by other authors are also included for comparison. In those studies, several techniques were employed, including low T series expansion [18, 19] and Monte Carlo simulation as well [21]. One can see that our data are fully compatible with the 3D Ising critical temperature (star symbol), which corresponds to the particular case M_k=0.

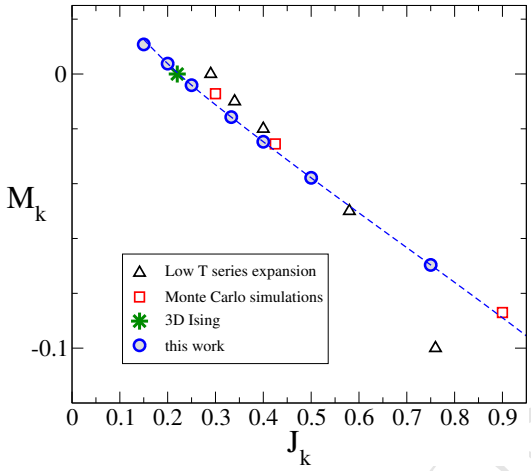

Figure 4: Partial phase diagram M_k-J_k of the Widom model focused on the region of the (continuous) order-disorder phase transition. Data taken from previous work correspond to critical points determined by different methodologies: Monte Carlo simulations (squares) and low-T series expansion (triangles). Our results (circles) allow us to delineate a phase edge for the transition (dashed line), which is compatible with the critical temperature of the 3D Ising model (star). The disordered and ordered phases are located below and above the line respectively.

4.4. Finite size scaling of thermodynamic magnitudes

Next, we will analyze the finite size behaviour of the magnetization, susceptibility and interfacial tension.

The critical behaviour of the magnetization depends on the critical exponent β. The finite size scaling given by Eq. 6 should collapse the magnetization m_L into a L-independent scaling function. Figure 5 shows a (logarithmic) scaling plot of the magnetization in which can be observed the collapse onto one master curve, assuming a critical exponent β and searching the adequate value of M_k^*. In the shown case, J_k=0.33, M_k^* results -0.015736 and the critical amplitude 1.455. As expected, the magnetization decreases at zero from two-phase region near the critical point.

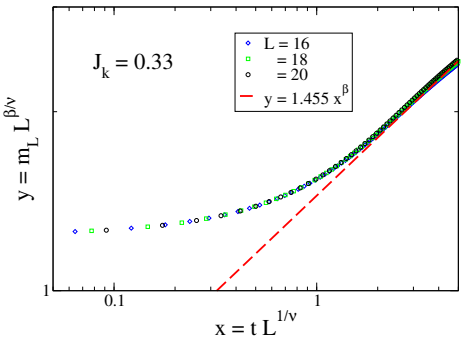

Figure 5: Scaling plot and collapse of the magnetization $m_{_L}$ for $J_{_k}$=0.33. The L-independent master curve is fitted by a power law with critical exponent β, from which results the critical amplitude B, as indicated.

The susceptibility $\chi_{_L}$ have a critical behaviour depending on the critical exponent γ. The application of Eq. 9 should also collapse it into a L-independent scaling function. In fact, scaling plots of Figs. 6*a,b* show the collapse of the susceptibility in the one-phase and two-phase regions respectively. Fig. 6*c* shows the susceptibilities $\chi_{_L}$ and the divergence of the critical curve χ_∞ from both sides of the critical point.

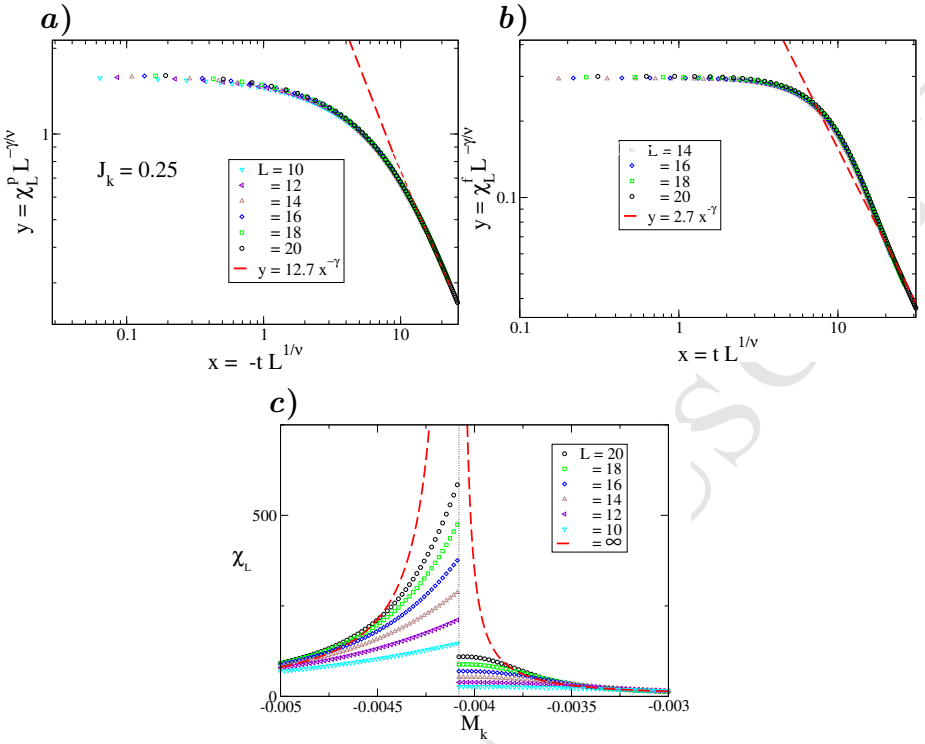

Figure 6: Scaling plots and critical behaviour of the susceptibility χ_L for J_k=0.25. Above, scaling plots of χ_L in the *a*) one-phase (χ_L^p) and *b*) two-phase (χ_L^f) regions. Master curves are fitted by power laws with critical exponent -γ, from which result the critical amplitudes Γ^+ and Γ^- respectively, as indicated. Below, *c*) susceptibilities χ_L^p and χ_L^f (symbols) with the corresponding critical curves (dashed line) as a function of M_k around the critical point.

Figure 7 shows the decaying of σ_L as the critical point is approximated from the two-phase region for J_k=0.33. As it can be seen, the interfacial tension extrapoled to the thermodynamic limit decays and becomes zero at critical point.

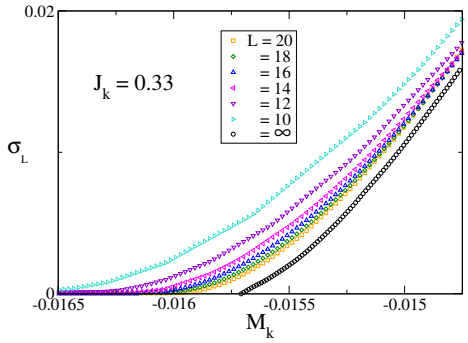

Figure 7: Interfacial tension σ_L and its extrapolation to the thermodynamic limit σ_∞ as a function of M_k for J_k=0.33. For each M_k value, data for different system sizes are extrapoled to the thermodynamic limit by fitting with the function of Eq. 12.

Figure 8 shows the critical behaviour of the interfacial tension for four of the J_k values analyzed. It can be noted error bars increase as the critical point is approximated from two-phase region. It is because the finite size effect requires simulating increasingly larger systems in order to maintain the fitting precision as the critical point is approximated, implying an increasing computational effort. However, as it can be seen in plots of Fig. 8, our simulation data up to L=20 still allow us to determine a critical behaviour, but up to a certain distance from the critical point. The power law behaviour with critical exponent 2ν reaffirm again the 3D Ising universality class.

Critical amplitudes σ_0 have an increasing behaviour at J_k values with criticality in the region M_k<0, as seen in plots of Fig. 8. As critical coupling parameters are increased in absolute value by following the phase transition line, the interface of these systems is more stable against thermal fluctuations. In the case of J_k=0.15, the critical point is located in the region M_k>0. That means each spin feels a ferromagnetic field that is contributed from first, second and fourth neighbors. The stability of the system is reinforced compared to the 3D Ising model, thus the creation of interfaces by thermal fluctuations is energetically less favorable.

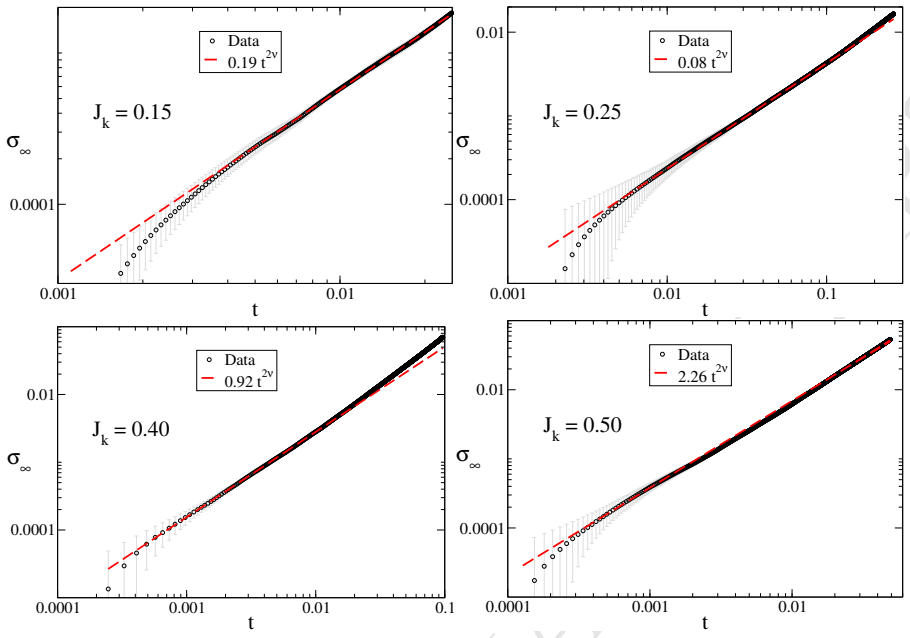

Figure 8: Critical behaviour of the interfacial tension σ_∞ for the different J_k values analyzed, as indicated. The variable t is the reduced M_k temperature. Error bars result from fits with Eq. 12 and are displayed in gray color. Dashed lines represent power law fits with critical exponent 2ν, resulting of them the critical amplitudes σ_0, as indicated.

Critical amplitude ratios

Once the critical amplitudes of the thermodynamic magnitudes of interest were calculated, these are used to test the universality by means of a number of ratios between them, Eqs. 3−5. In Table 2 we report the critical amplitudes ratios for the J_k values analyzed in this work. We emphasize that the errors, in both our and reference estimates, are significant due to the difficulty in general of measuring critical amplitudes. Within the error margin, we observe a reasonable agreement of our estimates with reference values of Eq. 3−5. Note that for the higher J_k values, 0.40 and 0.50, ratios exhibit a slight discrepancy with the reference values. The largest discrepancy are observed at first and third columns, ratios at first column are overestimated while at third column are

underestimated. Instead, ratios at second column are within the reference range, although the relative deviation to the reference value is greater than in the other columns. We believe the discrepancy could come from the estimation of the amplitudes Γ^- and B, since they are difficult of determining with precision due to the loses efficiency of Metropolis sampling within the two-phase region.

Table 2: Summary of critical amplitude ratios as obtained by finite size analysis for the J_k values analyzed. Reference values of Eqs. 3−5 are also listed for a best comparison.

J_k	Γ^+/Γ^-	$\sigma_0^{3/2}\Gamma^-/B^2$	$\sigma_0^{3/2}\Gamma^+/B^2$	
	4.52−5.00	0.09−0.17	0.58−0.89	Ref. [27]
0.20	4.54	0.1387	0.6292	
0.25	4.70	0.1307	0.5270	
0.33	4.79	0.1330	0.6009	this work
0.40	5.34	0.0969	0.5248	
0.50	5.55	0.1013	0.5797	

5. Conclusions

In summary, it has been achieved to obtain with precision the phase edge and to analyze in detail the critical behaviour of the order-disorder phase transition of the Widom model for microemulsions. We use a study strategy based on Monte Carlo simulations, combining a Metropolis sampling and multiple histogram reweighting technique.

In the phase diagram $M_k - J_k$, our critical points describe a phase transition line fully compatible with the known critical temperature of the 3D Ising model, which corresponds to a particular case of the Widom model (coupling parameter M=0). In addition, a rigorous finite size scaling analysis for thermodynamic magnitudes as magnetization, susceptibility and interfacial tension was performed, using the 3D Ising critical exponents. We achieve to obtain the critical amplitudes with a reasonable precision. Additionally, critical amplitudes were used to test the universality by means of a number of ratios belonging to the 3D

Ising universality class. Despite the difficulty in general of measuring critical amplitudes, we achieve to obtain ratios with a reasonable agreement.

In the next, we expect to approach a detailed study of the interfacial tension in the Widom model phase diagram. In that sense, we will resort to biased sampling techniques, as the so-called successive umbrella sampling (SUS) recently introduced by Virnau and Mller [34], which is more efficient than the sampling based on the Boltzmann distribution.

Acknowledgements

We acknowledge financial support from CONICET.

References

[1] J. Sjöblom, R. Lindberg, S. E. Friberg, Microemulsions phase equilibria characterization, structures, applications and chemical reactions, Advances in Colloid and Interface Science 65 (1996) 125–287. doi:10.1016/0001-8686(96)00293-X.
URL http://www.sciencedirect.com/science/article/pii/000186869600293X

[2] B. Widom, Lattice model of microemulsions, The Journal of Chemical Physics 84 (12) (1986) 6943–6954. doi:10.1063/1.450615.

[3] B. Widom, II. Theoretical modeling: An introduction, Berichte der Bunsengesellschaft für physikalische Chemie 100 (3) 242–251. arXiv:https://onlinelibrary.wiley.com/doi/pdf/10.1002/bbpc.19961000310, doi:10.1002/bbpc.19961000310.
URL https://onlinelibrary.wiley.com/doi/abs/10.1002/bbpc.19961000310

[4] I. W. Hamley, Introduction to soft matter: polymers, colloids amphiphiles, and liquid crystals, Wiley, Chichester; New York, 2000.

[5] T. A. Witten, Structured Fluids: Polymers, Colloids, Surfactants, Oxford University Press, 2004.
URL https://books.google.com.ar/books?id=uCwSDAAAQBAJ

[6] K. A. Dawson, Lattice Models of Amphiphilic Assembly, Springer Netherlands, Dordrecht, 1992, pp. 265–323. doi:10.1007/978-94-011-2540-6_13.

[7] G. Gompper, M. Schick, Correlation between structural and interfacial properties of amphiphilic systems, Phys. Rev. Lett. 65 (1990) 1116–1119. doi:10.1103/PhysRevLett.65.1116.
URL https://link.aps.org/doi/10.1103/PhysRevLett.65.1116

[8] G. Gompper, M. Schick, Lattice model of microemulsions, Phys. Rev. B 41 (1990) 9148–9162. doi:10.1103/PhysRevB.41.9148.
URL https://link.aps.org/doi/10.1103/PhysRevB.41.9148

[9] A. Ciach, J. S. Ho/ye, G. Stell, Bicontinuous phase in a lattice model for surfactant mixtures, The Journal of Chemical Physics 95 (7) (1991) 5300–5304. doi:10.1063/1.461668.

[10] K. Chen, C. Ebner, C. Jayaprakash, R. Pandit, Microemulsions in oil-water-surfactant mixtures: Systematics of a lattice-gas model, Phys. Rev. A 38 (1988) 6240–6254. doi:10.1103/PhysRevA.38.6240.
URL https://link.aps.org/doi/10.1103/PhysRevA.38.6240

[11] M. W. Matsen, D. E. Sullivan, Microemulsion and lamellar phases of a vector lattice model, Phys. Rev. E 51 (1995) 548–557. doi:10.1103/PhysRevE.51.548.
URL https://link.aps.org/doi/10.1103/PhysRevE.51.548

[12] M. Schick, W.-H. Shih, Spin-1 model of a microemulsion, Phys. Rev. B 34 (1986) 1797–1801. doi:10.1103/PhysRevB.34.1797.
URL https://link.aps.org/doi/10.1103/PhysRevB.34.1797

[13] M. Schick, W.-H. Shih, Simple microscopic model of a microemulsion, Phys. Rev. Lett. 59 (1987) 1205–1208. doi:10.1103/PhysRevLett.59.1205.
URL https://link.aps.org/doi/10.1103/PhysRevLett.59.1205

[14] K. Chen, C. Ebner, C. Jayaprakash, R. Pandit, Micro-emulsions in oil-water-surfactant mixtures: an ising lattice gas model, Journal of Physics C: Solid State Physics 20 (17) (1987) L361. doi:10.1088/0022-3719/20/17/001.
URL http://stacks.iop.org/0022-3719/20/i=17/a=001

[15] V. Privman, Fluctuating interfaces, surface tension, and capillary waves: an introduction, International Journal of Modern Physics C 03 (05) (1992) 857–877. doi:10.1142/S0129183192000531.

[16] K. A. Dawson, M. D. Lipkin, B. Widom, Phase diagram of a lattice microemulsion model, The Journal of Chemical Physics 88 (8) (1988) 5149–5156. doi:10.1063/1.454669.

[17] K. A. Dawson, Spatially frustrated lattice models, Phys. Rev. A 36 (1987) 3383–3391. doi:10.1103/PhysRevA.36.3383.
URL https://link.aps.org/doi/10.1103/PhysRevA.36.3383

[18] K. A. Dawson, B. L. Walker, A. Berera, Accounting for fluctuations in a lattice model of microemulsions, Physica A: Statistical Mechanics and its Applications 165 (3) (1990) 320–351. doi:10.1016/0378-4371(90)90003-B.
URL http://www.sciencedirect.com/science/article/pii/037843719090003B

[19] A. Berera, B. Kahng, Surface tension in the widom model by low-temperature expansion, Phys. Rev. A 46 (1992) 4528–4533. doi:10.1103/PhysRevA.46.4528.
URL https://link.aps.org/doi/10.1103/PhysRevA.46.4528

[20] G. Gompper, M. Schick, Microemulsion structure from a three-component lattice model, Phys. Rev. Lett. 62 (1989) 1647–1650. doi:10.1103/

PhysRevLett.62.1647.

URL https://link.aps.org/doi/10.1103/PhysRevLett.62.1647

[21] N. Jan, D. Stauffer, Monte carlo simulations of spin-1/2 micelle and microemulsion models, J. Phys. France 49 (4) (1988) 623–633. doi:10.1051/jphys:01988004904062300.

[22] D. Chowdhury, D. Stauffer, Amphiphilic membranes in thin films of a complex fluid: Statics and dynamics in lattice models, The Journal of Chemical Physics 95 (10) (1991) 7664–7677. doi:10.1063/1.461340.

[23] D. Chowdhury, D. Stauffer, Boundary effects on a spin-model: microemulsions in a confined geometry, Journal of Physics A: Mathematical and General 24 (12) (1991) L677.

URL http://stacks.iop.org/0305-4470/24/i=12/a=004

[24] A. M. Ferrenberg, R. H. Swendsen, Optimized monte carlo data analysis, Phys. Rev. Lett. 63 (1989) 1195–1198. doi:10.1103/PhysRevLett.63.1195.

URL https://link.aps.org/doi/10.1103/PhysRevLett.63.1195

[25] V. Privman, P. C. Hohenberg, A. Aharony, Universal critical-point amplitude relations, in: C. Domb, J. L. Lebowitz (Eds.), Phase Transitions and Critical Phenomena, Vol. 14, Academic Press, London, 1991.

[26] A. Pelissetto, E. Vicari, Critical phenomena and renormalization-group theory, Physics Reports 368 (6) (2002) 549–727. doi:10.1016/S0370-1573(02)00219-3.

URL http://www.sciencedirect.com/science/article/pii/S0370157302002193

[27] R. L. C. Vink, J. Horbach, K. Binder, Critical phenomena in colloid-polymer mixtures: Interfacial tension, order parameter, susceptibility, and coexistence diameter, Phys. Rev. E 71 (2005) 011401. doi:10.1103/

PhysRevE.71.011401.
URL https://link.aps.org/doi/10.1103/PhysRevE.71.011401

[28] D. Stauffer, M. Ferer, M. Wortis, Universality of second-order phase transitions: The scale factor for the correlation length, Phys. Rev. Lett. 29 (1972) 345–349. doi:10.1103/PhysRevLett.29.345.
URL https://link.aps.org/doi/10.1103/PhysRevLett.29.345

[29] K. Binder, E. Luijten, Monte carlo tests of renormalization-group predictions for critical phenomena in ising models, Physics Reports 344 (4) (2001) 179–253, renormalization group theory in the new millennium. doi:10.1016/S0370-1573(00)00127-7.
URL http://www.sciencedirect.com/science/article/pii/S0370157300001277

[30] H.-P. Deutsch, Optimized analysis of the critical behavior in polymer mixtures from monte carlo simulations, Journal of Statistical Physics 67 (5-6) (1992) 1039–1082. doi:10.1007/bf01049009.

[31] D. P. Landau, K. Binder, A Guide to Monte Carlo Simulations in Statistical Physics, Cambridge University Press, Cambridge, 2000. doi:10.1017/CBO9781139696463.

[32] K. Binder, Monte carlo calculation of the surface tension for two- and three-dimensional lattice-gas models, Phys. Rev. A 25 (1982) 1699–1709. doi:10.1103/PhysRevA.25.1699.
URL https://link.aps.org/doi/10.1103/PhysRevA.25.1699

[33] K. Binder, Finite size scaling analysis of ising model block distribution functions, Zeitschrift für Physik B Condensed Matter 43 (2) (1981) 119–140. doi:10.1007/BF01293604.

[34] P. Virnau, M. Mller, Calculation of free energy through successive umbrella sampling, The Journal of Chemical Physics 120 (23) (2004) 10925–10930. doi:10.1063/1.1739216.